High-frequency models of ferrite core inductorsProceedings of IECON'94 - 20th Annual Conference of IEEE Industrial Electronics

High–Frequency Models of Ferrite Core Inductors

M. Bartoli, A. Reatti*, Member, IEEE, and M. K. Kazimierczuk**, Senior Member, IEEE;

*University of Florence, Department of Electronic Engineering, Via di S. Marta, 3, 50139 Florence, Italy
Phone: (39)(55)4796–389 and Fax: (39)(55)494569. E – Mail: CIRCUITI@VM.IDG.CNR.FI

**Wright State University, Department of Electrical Engineering, Dayton, Ohio 45435
Phone: (513)873–5059 and Fax: (513)873–5009. E – Mail: MKAZIM@VALHALLA.CS.WRIGHT.EDU

Abstract **– A model of ferrite core inductors is presented. The skin and proximity effects which increase the ac resistance of the inductor winding are considered. The core losses are studied. Power losses of the inductor are modeled by means of a frequency dependent series resistance. Parasitic capacitances which affect the inductor high–frequency operation are also considered. The model is applicable to cores with and without an air gap. Calculated and measured inductor parameters such as equivalent series inductance (ESL), reactance, equivalent series resistance (ESR), impedance magnitude and phase, and quality factor are plotted as functions of the operating frequency and compared. Calculated results were in good agreement with the measured ones up to the inductor self–resonant frequency. As a consequence, the discussed model is suitable to represent the frequency response of ferrite core inductors and can be effectively used for designing inductors.**

I. Introduction

One method of reducing the overall size and weight of power converters is to increase the switching frequency above several hundred kilohertz. This allows the volumes of inductors, capacitors, and transformers to be much smaller. However, power converters can have small volumes only if a high efficiency is achieved at a high operating frequency. Therefore, parasitic resistances of the converter components should be as low as possible. Moreover, the parasitic components of passive and active devices used in the converter circuits must be accurately predicted to prevent unwanted behavior of the circuit. The dominant portion of the size of a power supply weight and/or volume belongs to its magnetic contents. Moreover, the parasitic resistances of inductors and transformers represent the major contribution of passive components to the power losses. Therefore, the optimization of the magnetic device design is crucial to increase the overall power density of the power converter circuits.

A high quality–factor inductor should have low copper and core losses and a high self–resonant frequency, that is, a low parasitic capacitance. Core losses are drastically reduced if distributed air gap cores with a low permeability, such as iron–powder cores, are used. However, multiple–turn and multilayer windings are necessitated to obtain the values of inductances required in power converters. This results in high parasitic capacitances and low self–resonant frequencies. Moreover, copper losses are high because of the length of the winding and skin and proximity effects which increase with number of layers in the coil winding. A lower number of turns is required if high–permeability cores are used. Unfortunately, these cores not only result in a relatively high power loss but also have a limited saturation flux density which requires an air gap to be introduced in the magnetic path. If the length of the gap is too large, the fringing flux near the air gap causes the total loss to increase. All aspects must be considered when designing a power converter. However, little on this topic can be found in available literature [1–13].

The purpose of this paper is to explore a model of soft ferrite core inductors in which parasitic capacitances as well as winding and core losses are taken into account. The skin and proximity effects that cause the high–frequency winding resistance to icrease are modeled by a frequency dependant resistance. The dependence of the ferrite core loss factor on frequency is also explored. Expressions for both the core and copper resistances as functions of the operating frequency and the inductor geometry are given. As a result, an accurate description of the frequency response of soft ferrite core inductors is achieved by means of a simple equivalent series model. A general procedure for extracting the inductor model components is also given. Therefore, the presented derivations can be easily extended to other inductors.

The significance of the paper is in that the discussed model allows all the parameters affecting the inductor quality factor to be accurately predicted and controlled during the inductor design. Therefore, this paper represents a contribution to the improvements of power inductor design and efficiency of power converters.

II. Ferrite Core Inductor Model

Fig. 1(a) shows the lumped parameter equivalent circuit of ferrite core inductors. Resitances R_w and R_{fc} are the winding and core resistances, respectively. Inductance L is the low–frequency inductance of the inductor and C is the overall parasitic capacitance including the distributed turn–to–turn, turn–to–core, and layer–to–layer capacitances. The winding resistance of the model depicted in Fig. 1(a) is [11]

$$R_w = R_{dc}A\left\{\frac{e^{2A}-e^{-2A}+2\sin 2A}{e^{2A}+e^{-2A}-2\cos 2A} + \frac{2\left(N_t^2-1\right)}{3}\frac{e^{A}-e^{-A}-2\sin A}{e^{A}+e^{-A}+2\cos A}\right\} \quad (1)$$

0-7803-1328-3/94$03.00© 1994 IEEE

where N_ℓ is the integer number of layers in the coil winding, R_{dc} is the dc inductor resistance at a given operating temperature, and [12]

$$A = \frac{\pi}{2}\sqrt{\frac{\sqrt{\pi}}{2}\frac{\mu_{rw}\mu_o d^3 f}{\rho t}} \tag{2}$$

f is the operating frequency in hertz, $\mu_o = 4\pi\ 10^{-10}$ H/mm, μ_{rw} is the conductor relative permeability, ρ is the conductor resistivity in Ωmm at a given operating temperature ($\rho = 17.24x10^{-6}$ Ωmm at a temperature $T = 20$ °C), d is the conductor diameter in mm, and t is the distance between the centres of two adjacent conductors in mm.

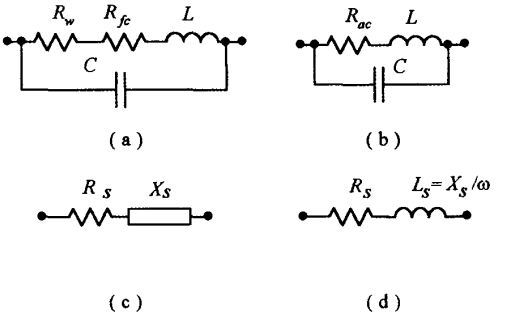

Fig. 1. Equivalent circuits of an inductor.
(a) Lumped parameter equivalent circuit.
(b) Simplified lumped parameter equivalent circuit.
(c) Equivalent series circuit.
(d) Equivalent circuit assumed by a LCR meter.

The core losses are taken into account by means of the core loss factor

$$tan\delta_m = tan\delta_e + tan\delta_r + tan\delta_h = tan\delta + tan\delta_h \tag{3}$$

where $tan\delta_e$, $tan\delta_r$, and $tan\delta_h$ are the eddy current, residual, and hysteresis loss factors, respectively. According to the soft ferrite core data books and IEC specifications, the hysteresis loss factor at a given ac magnetic flux density with an amplitude B_m is

$$tan\delta_h = \frac{tan\delta_{m2} - tan\delta_{m1}}{B_2 - B_1} B_m \tag{4}$$

where $tan\delta_{m1}$ and $tan\delta_{m2}$ are the core loss factors at magnetic flux densities of B_1 and B_2, respectively. The expression hysteresis loss factor given by (4) is valid for sinusoidal flux densities with a dc component $B_{dc} = 0$. If the current through the inductor is the combination of a dc component I_{dc} and an ac component with an amplitude I_m and the core is not operated in the saturation, the maximum flux density is expressed as

$$B_{tot} = B_{dc} + B_m = \frac{L I_{dc}}{N A_e} + \frac{L I_m}{N A_e} = \frac{L}{N A_e}(I_{dc} + I_m) \tag{5}$$

where B_{dc} is the dc component of the flux density and B_m is the amplitude of the ac component of the flux density. Only the ac component of the flux density contributes to the hysteresis loss and, therefore, to core resistance. With a nonzero component B_{dc}, the ac flux swing is moved toward saturation and one must check that the maximum flux density B_{tot} does not exceed the ferrite core saturation flux density B_{sat}. Moreover, hysteresis losses are reduced because only a portion of the overall BH loop is involved.

Since most of LCR meters allow only a low flux density operation of the tested inductor, the contribution of hysteresis losses to the core series resistance was neglected. Therefore, resistance R_{fc} of the circuit shown in Fig. 1(a) represents the small-signal resistance of the core and is independent of the flux density. The complex series permeability $\mu_s = \mu_s' + j\mu_s''$ allows the core loss factor to be expressed as

$$tan\delta_m = tan\delta = \frac{R_{fc}}{X_{fc}} = \frac{\mu_s''}{\mu_s'} = \alpha f^k \tag{6}$$

where X_{fc} is the core reactance and α and k are the multiplying coefficient and frequency exponent of the polynomial function giving the loss factor rise with frequency, respectively. Typical values of k for soft ferrite cores are in the range of 0.2–0.6; α is in the range 10^{-7}–10^{-5} s^k. From (6), the series core resistance is evaluated as

$$R_{fc} = X_{fc}\,\alpha f^k = 2\pi L \alpha f^{k+1}. \tag{7}$$

The inductance of a gapped core is

$$L = \frac{N^2}{\Re} = \frac{N^2}{\frac{l_e}{\mu_o \mu_r A_e}\left[1 + \mu_r \frac{l_g A_e}{l_e A_g}\right]} = A_L N^2 \tag{8}$$

where N is the number of turns of the winding, $\Re$ is the core reluctance (turns/H), A_e and A_g are the core and gap cross sectional areas given in square meters, respectively, l_e and l_g are the magnetic length of the core and gap in meters, μ_r is the core relative permeability with $l_g = 0$, and A_L is the inductance factor (typically given by ferrite core producers in nH/turn). Substitution of (8) into (7) gives

$$R_{fc} = 2\pi\mu_o \frac{\mu_r}{\left[1 + \mu_r \frac{l_g A_e}{l_e A_g}\right]} \frac{N^2 A_e}{l_e} \alpha f^{k+1}. \tag{9}$$

For a core with no air gap (9) simplifies as follows

$$R_{fc} = 2\pi\mu_o \frac{\mu_r N^2 A_e}{l_e} \alpha f^{k+1} = 8x10^{-7}\pi^2 \frac{\mu_r N^2 A_e}{l_e} \alpha f^{k+1}. \tag{10}$$

The total resistance of the model shown in Fig. 2(b) is

$$R_{ac} = R_w + R_{fc}$$

$$= R_{dc}A\left\{\frac{e^{2A}-e^{-2A}+2\sin 2A}{e^{2A}+e^{-2A}-2\cos 2A}+\frac{2\left(N_t^2-1\right)}{3}\frac{e^{A}-e^{-A}-2\sin A}{e^{A}+e^{-A}+2\cos A}\right\}$$

$$+8x10^{-7}\pi^2\frac{\mu_r}{\left[1+\mu_r\frac{l_g A_e}{l_e A_g}\right]}\frac{N^2 A_e}{l_e}\alpha f^{k+1}. \tag{11}$$

LCR meters measure the resistance and reactance of the impedance $Z_s = R_s + jX_s$ of the circuit shown in Fig. 1(c) when the series equivalent circuit model is selected. The equivalent series impedance of the circuit depicted in Fig. 1(a) is

$$Z_s = R_s + jX_s = |Z_s|e^{j\phi} \tag{12}$$

where

$$R_s = R_{ac}\frac{1}{\left(1-\omega^2 LC\right)^2+\omega^2 C^2 R_{ac}^2} \tag{13}$$

and

$$X_s = j\omega L\frac{1-\omega^2 LC-CR_{ac}^2/L}{\left(1-\omega^2 LC\right)^2+\omega^2 C^2 R_{ac}^2}. \tag{14}$$

By definition, the series reactance X_s is zero when the inductor is operated at the self–resonant frequency $f_r = \omega_r / 2\pi$. Since, in practice, $CR_{ac}^2/L << 1$, the parasitic capacitance C is found from (14) as

$$C = \frac{1}{\omega_r^2 L} = \frac{1}{(2\pi f_r)^2 L}. \tag{15}$$

The inductance L_s of the circuit shown in Fig. 1(d) is negative for $f > f_r$ because it is calculated by the LCR meter as

$$L_s = \frac{X_s}{\omega}. \tag{16}$$

The instruments calculate the inductor quality factor as

$$Q_s = \frac{|X_s|}{R_s}. \tag{17}$$

On the other hand, the ability of the inductor to store energy is described by defining a quality factor as

$$Q_o = 2\pi f\frac{E_L}{P_R} = \frac{\omega L}{R_{ac}} \tag{18}$$

where E_L is the maximum energy stored in the inductor and P_R is the power loss in inductor parasitic resistances.

III. Experimental Results

To verify the accuracy of the model, an inductor was assembled on a Philips 3F3 ETD44 ferrite core with no air gap. The core cross sectional area was A_e = 176 mm^2, the magnetic path length l_e = 103 mm, the relative permeability μ_r = 1800, and inductance factor A_L = 3200 nH. A solid copper round wire with d = 0.56 mm and t = 0.61 mm was wound using $N_t = 2$ and $N = 90$. The inductance calculated from (8) was L = 25.5 mH. The number of turns that can be wound over one layer is

$$N_{TL} = \frac{l_w}{t}. \tag{19}$$

where l_w is the winding with of the coil former. Since l_w = 29.5 mm for an ETD44 coil former, (19) gives N_{TL} = 48 turns. The measurements were performed using a HP 4192/A LCR meter equipped in test fixture HP 16047/A to minimize the residual parameters. Fig. 2(a) shows a plot of measured reactance X_s. Reactance X_s was equal to zero at $f = f_r$ = 100 kHz. Since the low frequency inductance was L = 25.5 mH, (15) yields C = 105.65 pF. The equivalent series resistance measured at a low operating frequency R_s = 2.2 Ω was chosen as the value of R_{dc}. Using accurate measurements at 30 kHz and 50 kHz, the values of α and k were calculated as $1.33x10^{-5}$ s^k and 0.5, respectively.

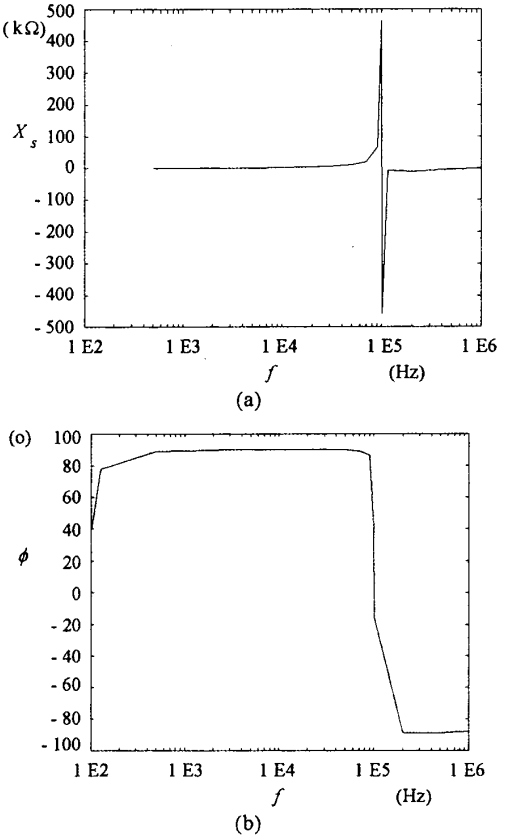

Fig. 2. Inductor measured equivalent series impedance.
(a) Reactance X_s versus frequency f.
(b) Phase ϕ versus frequency f.

Fig. 2(b) shows a plot of the measured phase of the impedance. According to the definition of the self–resonant frequency,

phase ϕ abruptly changes from positive values close to 90° to negative values at f = 100 kHz.

Fig. 3 shows the plots of the core resistance R_{fc}, the winding resistance R_w, and total resistance of the model R_{ac} as functions of frequency. The core resistance contributes to the rise of the total resistance over the entire frequency range while skin and proximity effects do not affect the inductor resistance for frequencies up to 20 kHz.

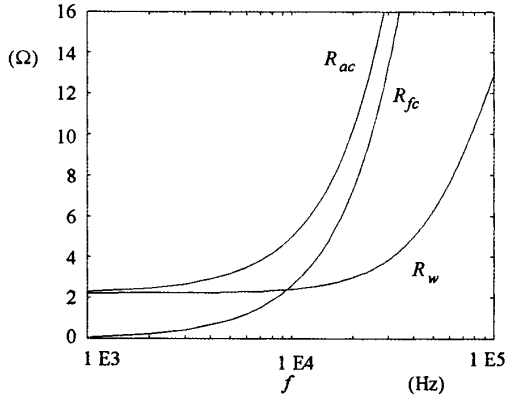

Fig. 3. Core resistance R_{fc}, winding resistance R_w, and total inductor resistance R_{ac} versus frequency f.

The total ac resistance of the inductor and equivalent series resistance R_s are compared in Fig. 4. Since they have the same values up to 20 kHz frequency, we can conclude that the self-resonance does not affect the inductor parasitic resistance up to 20% of the self-resonant frequency, that is, up to a frequency where the total series resistance of the inductor is ten times higher than at f = 1 kHz.

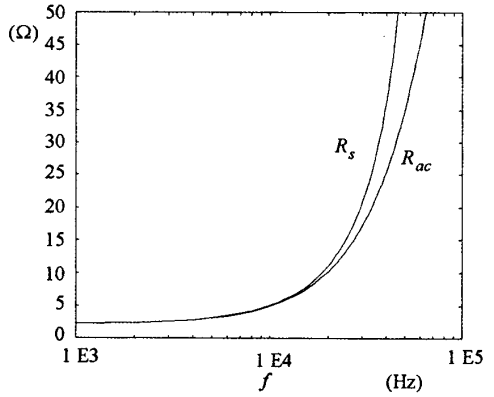

Fig. 4. Equivalent series resistance R_s and total inductor resistance R_{ac} versus frequency f.

The measured and calculated equivalent series resistances are compared in Figs. 5 and 6. The predicted and measured values of R_s are in good agreement up to the self-resonant frequency f_r. Figs. 7 and 8 show that also the measured and calculated reactances are practically identical for $f < f_r$. Plots of the measured quality factor and that calculated from (17) are depicted in Fig. 9. Both plots agree up to the self-resonant frequency. Calculated and measured plots of quality factor Q_o are compared in Fig. 10. Calculated and measured Q_o are nearly equal up to f = 40 kHz. At higher operating frequencies Q_o slowly decreases to zero because the energy stored in the inductor parasitic capacitances was not considered in (18). The calculated and measured inductor quality factors have a maximum value at f = 10% of the self-resonant frequency.

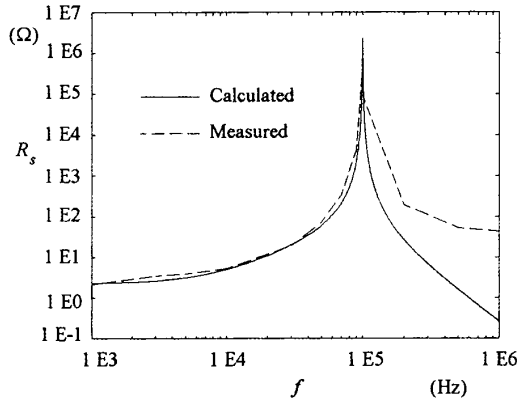

Fig. 5. Measured and calculated equivalent series resistance R_s versus frequency f.

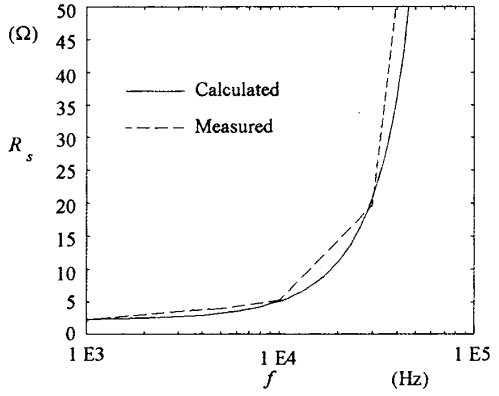

Fig. 6. Detailed plots of the measured and calculated equivalent series resistance R_s versus frequency f below self-resonant frequency.

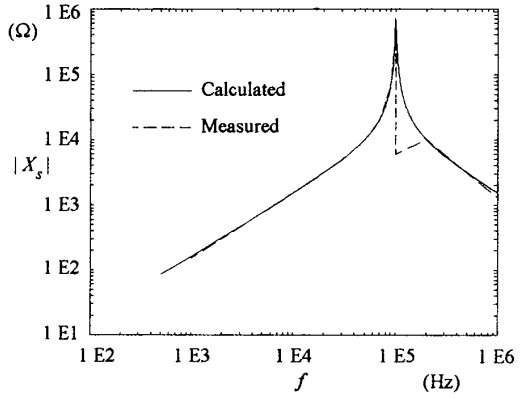

Fig. 7. Absolute values of the measured and calculated equivalent series reactance X_s versus frequency f.

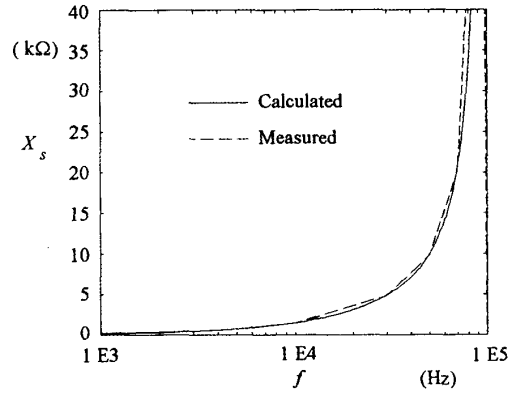

Fig. 8. Detailed plots of the measured and calculated equivalent series reactance X_s versus frequency f below self–resonant frequency.

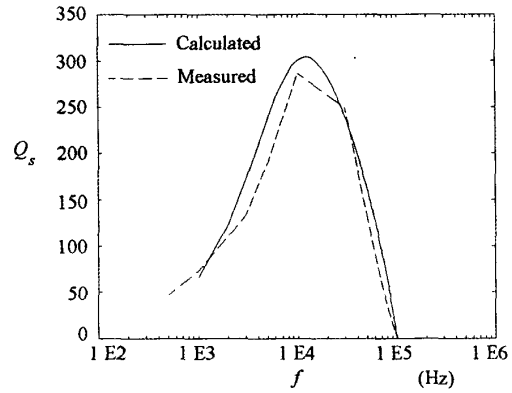

Fig. 9. Measured quality factor Q_s and calculated quality factor $Q_s = X_s/R_s$ versus frequency f.

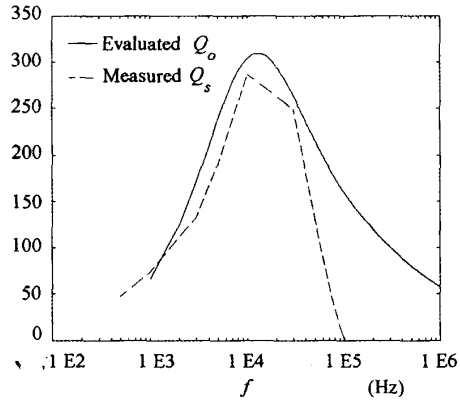

Fig. 10. Measured quality factor Q_s and calculated quality factor $Q_o = \omega L_s / R_{ac}$ versus frequency f.

The maximum amplitude of a sinusoidal current with no dc component which can flow through an inductor without core saturation is given by

$$I_m = \frac{NA_e B_{sat}}{L} \tag{20}$$

where I_m is in ampere when the soft ferrite core saturation flux density B_{sat} is in Tesla (B_{sat} = 220 mT for a 3F3 ferrite core), A_e is given in m^2, and L in H. From (20), the maximum current amplitude with N = 90, A_e = 176 mm^2, and L = 25.5 mH is I_m = 136 mA. At an operating frequency f = 30 kHz the core and winding resistances are R_{fc} = 7.27 Ω and R_w = 2.9 Ω, respectively. This results in a power loss P_{fc} = 134 mW and P_w = 54 mW in the core and winding resistances, respectively. This is, core loss is about three times higher than winding loss. Note that R_{fc} is the core small signal resistance. The actual core resistance depends on the core operating flux density and should be calculated considering the contribution of (4). This contribution is drastically reduced if a core with an air gap is used. A higher number of turns is required to achieve the same inductance value and the flux density the core is operated at is reduced. Assuming that a core with an air gap with l_g = 0.1 mm is used. From (8) an inductance factor A_L = 1400 is calculated assuming $A_e = A_g$. To achieve an inductance L = 25.5 mH a solid round wire with d = 0.56 mm and t = 0.61 mm must be wound using N = 134 and N_ℓ = 3. The maximum flux density the inductor is operated at is decreased to B_m = 147 mT, that is, 1.5 times lower than with N = 90. The small–signal core resistance is as high as before and from (1), the winding resistance is calculated as R_w = 23.68 Ω. If the air gap length is increased to l_g = 0.8 mm, the inductance factor decreases to A_L = 320, the number of turns increases to N = 282, and the maximum flux density is reduced to B_m = 70 mT. If the same solid copper round wire is used, the number of layers increases to N_ℓ = 6. This yields a winding resistance R_w = 66.07 Ω and a winding power loss P_w = 1.23 W. The hysteresis loss is further reduced. The expression of R_{fc} as a function of B_m and f should be determined to calculate the overall power loss in the inductor core.

IV. Conclusions

An equivalent lumped parameter circuit of soft ferrite core inductors has been discussed. Turn–to–turn, layer–to–layer, and layer–to–core capacitances have been considered along with their contribution to the inductor self–resonant frequency. The increase of the winding parasitic resistance with frequency and coil winding structure have been taken into account. Variations of the ferrite core complex permeability with frequency have also been considered. As a result, the expressions of inductor equivalent resistance and reactance have been derived. Theoretical plots of inductor resistance, reactance, and quality factor have been drawn and compared with those obtained by experimental tests. Theoretical and experimental results were in good agreement over a frequency range up to the inductor self–resonant frequency; that is, over a frequency range wider than that where the inductor can be properly operated. A capacitive reactance of the model is

obtained for operating frequencies higher than the self–resonant frequency, according to the results of the experimental tests. Both the calculated and the measured inductor quality factor have a maximum at a frequency equal to 10 % of the self–resonant frequency. Moreover, it has been demonstrated that the effect of the self–resonance does not affect the inductor parasitic resistance up to 20% of the self–resonant frequency. Therefore, the parasitic capacitances do not affect the inductor ESR for frequencies up to the frequency at which the inductor quality factor decreases to 80% of its maximum value. At this frequency, the inductor total series resistance is ten times higher than at $f = 1$ kHz.

It has been shown that ferrite cores with no gaps result in high ac resistances which highly depend on the operating frequency. For frequencies above 10% of the self–resonant frequency, the core resistance represents the major contribution to the overall ac resistance. Core resistances can be reduced if an air gap is introduced in the magnetic path. This also contributes to increase the self–resonant frequency. However, if the air gap length is too long, the fringing flux effect in not negligible and produces higher power losses in the core and in the winding. For this reason, the air gap length should not exceed 0.7–1% of the magnetic path length. As a consequence, iron–powder cores should be used at high–operating frequency. It has been observed that inductors in resonant power converters assembled on ferrite and iron–powder cores have similar dimensions and power losses when operated in a frequency range of 300–600 kHz. At higher frequencies, iron–powder cores perform better than ferrite cores even if they allow for low inductance values to be achieved .

The inductor model can be effectively used to design high–quality factor inductors, thus allowing power converters to be operated at a high–frequency with a high–efficiency. The model discussed in this paper is also suitable for time and frequency domain computer simulations of power converter circuits.

REFERENCES

[1] C. Wm. T. Mc. Lymann, *"Transformer and Inductor Design Handbook"*, New York: Marcel Decker Inc., 1978.

[2] Colonel Wm. T. Mc. Lymann, *"Magnetic Core Selection for Transformers and Inductors"*, New York: Marcel Decker Inc., 1982.

[3] W. J. Moore and P. N. Miljanic, *"The Current Comparator"*, United Kingdom: Peter Peregrinus Ltd., 1988.

[4] O. Kiltie, *"Design Shortcuts and Procedures for Electronic Power Transformers and Inductors"*, Cleveland,: Harris Publishing Company, 1975.

[5] W. M. Flanagan, *"Handbook of Transformer Applications"*, New York: Mc. Graw Hill, 1986.

[6] N. R. Grossner, *"Transformers for Electronic Circuits"*, Second Edition, New York: Mc. Graw Hill, 1983.

[7] R. Lee, L. Wilson, and C. E. Carter, *"Electronic Transformers and Circuits"*, Third Edition, New York: John Wiley and Sons, 1988.

[8] M. K. Jutty, V. Swaminathan, and M. K. Kazimierczuk, *"Frequency Characteristics of Ferrite Core Inductors"*, Proc. of *the Electrical Manufacturing & Coil Winding Symposium '93*, Chicago, IL, 1993, pp 369–372.

[9] J. R. Fluke, *"Controlling Conducted Emission by Design"*, New York: Van Nostrand Rehinold, 1991.

[10] K. H. Billings , *"Switchmode Power Supply Handbook"*, New York: Mc. Graw Hill, 1989.

[11] P. L. Dowell, *"Effects of eddy current in transformer windings"*, Proc. IEE, Vol. 113, No. 8, August 1966, pp. 1287–1394.

[12] J. Jongsma, *"High Frequency Ferrite Power Transformer and Choke Design" – Part 3 "Transformer Winding Design"*, Philips Technical Publication 207, Ordering code: 939805330011.

[13] Hewlett–Packard Co., *LCR Meter Model 4192/A Operating Manual.*